Available online at www.sciencedirect.com

ScienceDirect

Green Energy & Environment 6 (2021) 138–149

www.keaipublishing.com/gee

Research paper

Cross-polymerization between the model furans and phenolics in bio-oil with acid or alkaline catalysts

Qing Xu [a], Xun Hu [a,*], Lijun Zhang [a], Kai Sun [a], Yuewen Shao [a], Zhiran Gao [a], Qing Liu [b], Chun-Zhu Li [c,*]

[a] School of Material Science and Engineering, University of Jinan, Jinan, 250022, China

[b] Key Laboratory of Low Carbon Energy and Chemical Engineering, College of Chemical and Environmental Engineering, Shandong University of Science and Technology, Qingdao, 266590, China

[c] Fuels and Energy Technology Institute, Curtin University, GPO Box U1987, Perth, WA, 6845, Australia

Received 31 October 2019; revised 4 March 2020; accepted 23 March 2020
Available online 2 April 2020

Abstract

Polymerization is a major challenge for the upgrading of bio-oil to biofuels, but is preferable for the production of carbon material from bio-oil. Understanding the mechanism for polymerization is of importance for tailoring property of carbon material. This study investigated the characteristics for the polymerisation of furfural, vanillin, their cross-polymerization and the impacts of catalysts on their polymerization. The results indicated that the organic acids like acetic acid and formic acid could catalyze the polymerisation of furfural, while H_2SO_4 or NaOH as catalyst could drastically enhance the degree of polymerization of furfural. Vanillin showed a higher tendency towards polymerization than furfural and H_2SO_4 or NaOH significantly facilitated the polymerization of vanillin via shifting the pasty product to solid polymer. The cross-polymerization between furfural and vanillin occurred even in the absence of catalyst, while the presence of H_2SO_4 or NaOH catalyst resulted in the formation of more solid polymer via cross-polymerization. The polymerisation reactions were accompanied with the consumption of –C=O via aldol addition/condensation reactions. In addition, the morphology and thermal stability of the polymers formed were affected by both the type of the catalysts employed, which can in turn enhance the cross-polymerization between furfural and vanillin.

Keywords: Furfural; Vanillin; Cross-polymerization; Catalysts; Polymers

1. Introduction

Bio-oil is a condensable liquid produced from the pyrolysis of biomass, which has a complex composition. The main components of bio-oil include approximately three main categories. The carbohydrates and their derivatives, including sugar monomers and oligomers, are formed via the degradation of cellulose and hemicellulose [1–8]. The derivatives of carbohydrates, including furans, aldehydes, ketones and carboxylic acids [1,9,10], are formed from the scission of the aliphatic structures in cellulose/hemicellulose via reactions such as retro-aldol condensation [11–13]. The phenolics, including the phenolic monomers and oligomers, are mainly derived from the degradation of lignin, while, during pyrolysis, some derivatives of cellulose/hemicellulose could also form phenolics via aromaticisation [14–18]. These organic components have distinct structures with varied functionalities such as hydroxyl groups, aldehyde groups, ketone groups, carboxylic groups, ether groups, ester groups and conjugated π-bond structures. These organics are very reactive, especially towards polymerization, which is the origin of the unstability of bio-oil [19]. The high tendency of bio-oil towards polymerization represents a major

* Corresponding authors.
E-mail addresses: Xun.Hu@outlook.com (X. Hu), chun-zhu.li@curtin.edu.au (C.-Z. Li).

https://doi.org/10.1016/j.gee.2020.03.009

challenge for upgrading via hydrotreatment at elevated temperatures [20,21]. Great efforts have been made to tackle the polymerization of bio-oil, such as the pretreatment of bio-oil via esterification [22,23], the development of the various types of catalysts [24–26] and the optimization of the design of reactor configurations [27]. Nevertheless, polymerization of bio-oil is still a bottle-neck issue to be resolved.

Alternatively, we can consider bio-oil as a precursor for the formation of carbon material. The polymerization of bio-oil would no longer be a problem to be avoided, but a preferred reaction route. We have developed a technology for the polymerization of bio-oil, especially with the aid of furfural to produce a high yield of carbon material from biomass [28,29], which has great application prospects in some industrial sectors, such as metallurgical coke used in the iron and steel industry and electrodes used in the aluminium industry. The carbon materials prepared by the polymerization of bio-oil could also possibly used for preparation of catalysts, super capacitor, absorbents, etc. Nevertheless, the reaction network during the polymerization of bio-oil/furfural mixture has not yet been clarified, especially the role(s) of furfural during the polymerization.

Furfural is reactive towards polymerization [29,30]. Its furan ring can be attacked by an electrophile via an electrophilic substitution reaction, while the existence of the aldehyde group makes the molecule also reactive in aldol condensation reactions [29]. More importantly, the opening of the furan rings can produce some even more reactive sites for polymerization. However, the contribution of furfural to the polymerization of the complex mixture of organics in bio-oil is still unclear.

Bio-oil contains not only abundant organic compounds that are prone to polymerization, but also abundant carboxylic acids (i.e. formic acid, acetic acid, propionic acid, etc) that might act as catalysts for polymerization [31]. Nevertheless, it has not yet been clear if the carboxylic acids in bio-oil could promote the polymerization of furfural with the main components of bio-oil. In order to fill this knowledge gap, the polymerization of furfural in the absence of acids and in the presence of H_2SO_4, NaOH, formic acid, acetic acid was investigated in this study. Furthermore, the effects of the acid/alkaline catalysts on the cross-polymerization between furfural and vanillin, a typical phenolic compound in bio-oil, were also investigated. The liquid and solid products formed were analyzed in detail and the impacts of the acid/alkaline catalysts on the polymerization of furfural or vanillin and the cross-polymerization between furfural and vanillin were a key focus of this study.

2. Experiments and methods

2.1. Materials

Furfural and vanillin were purchased from Shanghai Macklin Biochemical Co., Ltd., China, H_2SO_4, NaOH, formic acid (FA) and acetic acid (AA) produced by China Pharmaceutical Group Chemical Reagents Co., Ltd. were used as catalysts for the polymerization of furfural or vanillin, which are analytic grade.

2.2. Experimental procedures

Furfural, vanillin or the mixture of furfural and vanillin (the molar ratio of 1:1) were respectively used as feedstock. H_2SO_4, NaOH, formic acid and acetic acid were used as catalysts for the polymerization. The loading of the catalyst was adjusted to achieve 0.0048 mol H^+ or OH^- in the reaction medium. It needs to note that the 0.0048 mol of formic acid or acetic acid were used even though the hydrogen ions cannot fully release in these organic acids. 4 mL of deionized water was used as reaction medium. The rationale for using water as a solvent was to disperse furfural, vanillin and the homogenous catalysts, as vanillin was a solid material at room temperature. In addition, bio-oil contains abundant water and therefore water as the reaction media was more suitable for analogy of the polymerisation of the main components in bio-oil. After mixing and loading the all substances at room temperature, the autoclave (10 mL in volume) was assembled and flushed with N_2 for three times to remove the residual O_2 in the reactor vessel. After that, the reactor was pressurized to 30 bar, while the temperature was raised to 200 °C in 30 min and then held for 4 h with a stirring rate of 400 rpm min^{-1}. The reason why the reaction was carried out under high temperature and pressure was to prepare high yield carbonaceous materials by using the properties of bio-oil which was easy to polymerize, which is conducive to the following research and future application. After finishing the experiments and cooling down of the reactor to room temperature, the liquid and solid products were collected separately. Owing to the different degree of the polymerization, some liquid products were stratified. The supernatant liquid and the viscous paste in bottom were separated via filtration. The solid products were defined as polymers. The definitions of the conversion of furfural or vanillin and the yield of polymer were shown below.

$$\text{Conversion (\%)} = \text{Mole of furfural (vanillin) converted/Mole of furfural (vanillin) loaded} \times 100\%$$

$$\text{Yield (\%)} = \text{Weight of polymer formed/Weight of reactant loaded} \times 100\%$$

2.3. Analytical methods

2.3.1. Gas chromatography–mass spectrometry (GC–MS)

The liquid products were analyzed with GC–MS (Shimadzu QP2020) with a DB wax capillary (length: 30 m; inner diameter: 0.25 mm). The sample was diluted with acetone with a mass ratio of 50 : 1, and then the diluted sample of 0.5 μL was injected into the 250 °C of injection port. The column heating procedure refers to our previous study [32]. Helium with a flow rate of 4 mL min^{-1} was used as carrier gas.

2.3.2. UV-fluorescence spectroscopy

The liquid products were characterized by using a UV-fluorescence spectrometer (Shimadzu RF6000), aiming to detect the conjugated π-bond structures formed during polymerization. The liquid samples were diluted to 400 ppm in methanol, which was within the linear range of the response of the signal to abundance of the conjugated π-bond structures in the products. The excitation wavelength started at 220 nm with the emission wavelength ranged from 250 to 500 nm to obtain a 2D synchronous spectrum. In addition, the excitation wavelength was also varied from 200 to 400 nm with the emission wavelength ranging from 220 to 500 nm to obtain a 3D synchronous spectrum. Different conjugated π-bond structures correspond to distinct wavelengths in the spectrum, which was further indicated with measuring the standard compounds.

2.3.3. High performance liquid chromatography (HPLC)

The water-soluble macromolecules in the liquid products were separated by gel filtration chromatography (GFC) to calculate the relative molecular weight of soluble oligomers in liquid products with HPLC (LC-20AD/T LPGE kit). The gel chromatographic column (Asahipak GF-310 HQ) was used with a column temperature of 35 °C. The deionized water was used as mobile phase with a flow rate of 0.4 mL min^{-1}. According to the fitting curve of maltose standard, the relative molecular weight of soluble oligomer was calculated.

2.3.4. Fourier-transform infrared spectroscopy (FT-IR)

FT-IR (NICOLITE IS50) was used to measure the functionalities in the products. For the liquid or paste samples, the ATR accessories were used for the analysis. The liquid or paste was loaded into the detection window, and then the probe was tightened to make the sample close to the probe for detection. Besides, the solid polymers were mixed with KBr at the ratio of 1:199, ground evenly and then dried at 105 °C for 4 h before pressing to a tablet of disc shape for the test.

2.3.5. Scanning electron microscope (SEM)

SEM (Phenom, ProX, Netherland) was used to observe the morphology of the polymers. The sample was bonded to the conductive adhesive, and then, it was sprayed with gold before the observation.

2.3.6. Thermo gravimetric analysis (TGA)

The thermal stability of the polymer was measured with a TGA (Rigaku TG8121). The polymer was heated at a crucible made of Al_2O_3 in a nitrogen flow (70 mL min^{-1}). The heating procedure refers to our previous study [32].

2.3.7. Extraction test

The solubility of polymers in organic solvent could be a rough indicator of the degree of the polymerization. Thus, the extraction of the polymer with acetone was carried out. 0.15 g of polymer was dissolved in 3 g of acetone and stirred for 30 min. After that, the liquid and residual solid were filtered and separated. The undissolved polymer was dried at 35 °C for 4 h until it reached a constant weight. The solubility here was defined as the following equation.

$$\text{Solubility (\%)} = \text{Weight of the polymer decreased/Weight of the polymer loaded} \times 100\%$$

3. Results and discussion

3.1. Effect of catalyst on the conversions of feedstock and the yields of products

Table 1 shows the conversion of furfural and vanillin as well as the distribution of the main products. In the absence of catalyst, the thermal treatment also led to the conversion of furfural with the formation of polymer and pasty material as the main products (Entry 5, Table 1). The use of acetic acid did inhibit the conversion of furfural, however, the yield of polymer and the amount of pasty material increased (Entry 4, Table 1). Formic acid could remarkably promote the conversion of furfural via forming more polymers (Entry 3, Table 1). This is related to the higher acidity of formic acid than acetic acid. The use of H_2SO_4 as catalyst further promoted the degree of the polymerization of furfural owing to the polymer as the main product (Entry 1, Table 1). Higher acidity clearly promoted the polymerization of furfural. In addition, the strong alkaline, NaOH, could also effectively catalyze the polymerization of furfural (Entry 2, Table 1). Furfural could polymerize via opening of the furan ring and the subsequent aldol condensation reaction [33], while the aldol condensation reactions could be catalyzed by both acid and alkaline [34,35].

Vanillin was more reactive towards polymerization than furfural. As shown in Entry 10, Table 1, in the absence of acid catalyst, 90.5% of vanillin could be converted and the pasty materials were formed via the polymerization as the main products. The organic acids (formic acid and acetic acid) seemed to have little influence on the degree of the polymerization of vanillin, except the slight increasing of the conversion, as pasty material was produced as the main product and no solid polymer was formed (Entry 8 and 9, Table 1). In the presence of H_2SO_4 or NaOH, the degree of the polymerization of vanillin was clearly enhanced, shifting the main product from pasty material to solid polymer (Entry 6 and 7, Table 1). Except for polymerization, with the presence of the strong acid/alkaline catalysts, the cracking of the carbonyl functionality also took place, producing a small amount of guaiacol.

The polymerization of furfural and vanillin was also focused via the investigation of the conversion of furfural and vanillin together. In the absence of catalyst, the conversion of furfural in the mixture was much higher than that in conversion of furfural alone (83.9% vs. 40.0%). Vanillin and furfural could polymerize together. Further to this, with the presence of organic acids, the mixture of furfural and vanillin was mainly converted into pasty material. In comparison, both acetic acid and formic acid could catalyze the conversion of furfural itself into solid polymer (Entry 3 and 4, Table 1). Vanillin could clearly interfere the polymerization of furfural. Further

Table 1
The conversion of feedstock and the yield of guaiacol under the different catalysts[a].

Entry	Sample	Conversion of F[b] (%)	Conversion of V[c] (%)	Yield of guaiacol (%)	Yield of polymer (%)	Weight of paste (g[d])
1	F−H_2SO_4	98.8	–	–	85.1	–
2	F−NaOH	94.1	–	–	82.9	–
3	F-FA	83.2	–	–	40.3	–
4	F-AA	26.5	–	–	10.7	1.5
5	F	40.0	–	–	5.8	0.88
6	V−H_2SO_4	–	97.3	0.60	82.9	–
7	V−NaOH	–	98.8	0.51	87.5	–
8	V-FA	–	97.0	0.01	–	3.1
9	V-AA	–	94.6	0.01	–	4.3
10	V	–	90.5	0.01	–	3.0
11	F−V−H_2SO_4[e]	99.8	98.8	0.22	91.3	–
12	F−V−NaOH	99.4	98.2	0.66	100.0	–
13	F−V-FA	83.0	92.2	0.01	–	3.3
14	F−V-AA	80.1	90.9	0.01	–	3.8
15	F−V	83.9	94.1	0.01	–	3.3

[a] Reaction conditions: Furfural, vanillin and the mixture of furfural and vanillin (with the molar ratio of 1:1) loaded each: 4 g; Catalysts (H^+ or OH^-) loaded each: 0.0048 mol; Deionized water: 4 mL; Reaction temperature: 200 °C; Reaction time: 4 h; Pressure: 30 bar. The yields of the polymer shown in the tables were generally within the experimental error of ±2%.
[b] F represents that the feedstock is furfural.
[c] V represents that the feedstock is vanillin.
[d] Paste is denoted by weight, because it is viscous liquid containing a lot of water and meaningless to calculate the yield.
[e] F–V–H_2SO_4: F–V represents that feedstock is the mixture of furfural and vanillin, and then H_2SO_4 is the catalyst.

evidence could be observed for the polymerization of the mixture of furfural and vanillin. The yields of solid polymer (Entry 11 and 12, Table 1) were higher than that in the conversion of the individual furfural (Entry 1 and 2, Table 1) or vanillin (Entry 6 and 7, Table 1) in the presence of the strong alkaline or strong acids. The results herein indicated, obviously, with or without the acids or alkaline as catalyst, the cross-polymerization between furfural, a typical sugar derivative in bio-oil, and vanillin, a typical derivative from lignin, existed and led to the formation of more solid polymer.

3.2. Characterization of the conjugated π-bonds of the liquid products and pastes with UV-fluorescence

Fig. 1 shows the UV-fluorescence synchronous spectra for the residual liquid after the conversion of furfural and vanillin. Generally, the molecules with π–π* and n–π* transition structures produced the fluorescence at certain excitation and emission wavelengths. Most fluorescent substances contained the conjugated π-bonds such as aromatic rings or heterocycles (such as furan rings). The wavelength generally corresponded to the size of the conjugate π-bonds [36]. For comparison, the UV-fluorescence synchronous spectra of standard chemicals were also measured under the similar conditions and the results were shown in Figure S1.

In the liquid products, in addition to the unconverted furfural and vanillin, there was also soluble oligomer with larger molecular sizes (Fig. 1a–c). Further polymerization of these soluble oligomer resulted in the formation of the pasty material that was an intermediate for the further transition to insoluble polymer. These substances contained conjugated π-bonds with varied size and abundance, as evidenced by the fluorescence spectra (Fig. 1d).

In the presence of H_2SO_4, the fluorescence peak for the soluble oligomer produced from the polymerization of furfural centered at about 300 nm (Fig. 1a), which was attributed to the conjugated π-bonds in furan, while the fluorescence of furfural peaked at ca. 329 nm (Fig. S1a). The condensation reaction via aldol condensation always led to the formation of conjugated π-bonds with a bigger size. Nevertheless, the polymerization of furfural here also included the reactions that could eliminate the carbonyl group in furfural. In addition, the polymerization of furfural also led to the formation of the polymers with larger conjugated π-bonds, as evidenced by the peaks located at 360 and 405 nm (Fig. 1a). With NaOH as catalyst, the intensity of the fluorescence peak for the soluble oligomer from furfural was lower, while the distribution of the wavelength was similar. With the organic acids as catalysts, the fluorescence intensity was relatively low. The organics should be mainly transformed into the pasty phase or they contained the electron-withdrawn functionality that weakened the fluorescence intensity.

For vanillin, the compound itself has a fluorescence peaked at ca. 364 nm (Fig. S1c), while during the polymerization of vanillin in the presence/absence of catalysts, the peak at 300 nm was very significant (Fig. 1b). The polymerization of vanillin also involves the cracking to form smaller conjugated π-bonds. For the polymerization of the mixture of furfural and vanillin, the fluorescence spectrum was similar while the distribution of the peaks was also similar (Fig. 1c). The pasty materials formed from the polymerization of furfural in the absence of catalyst and in the presence of acetic acid were also measured. The fluorescence spectrum mainly peaked at 360, 380, 420 and 460 nm (Fig. 1d). The conjugated π-bonds in the pasty materials were much larger than that in the liquid products.

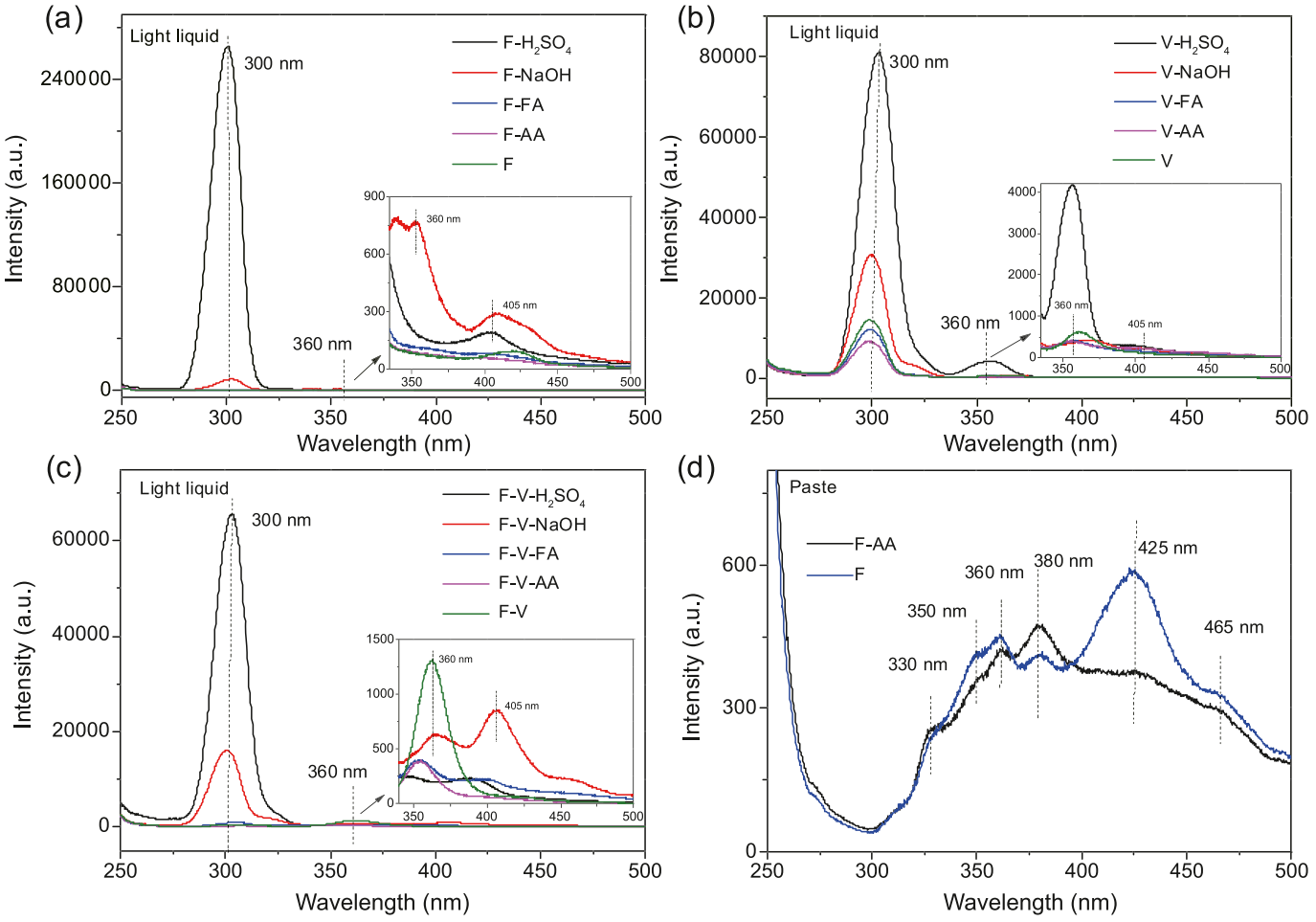

Fig. 1. UV-fluorescence synchronous spectra of liquid products and pastes produced via the polymerization. (a) Liquid products obtained with furfural as reactant; (b) liquid products obtained with vanillin as reactant; (c) liquid products obtained with the mixture of furfural and vanillin as reactant; (d) pastes obtained with furfural as reactant. All samples were diluted to 400 ppm by methanol.

The 3D UV-fluorescence synchronous spectra can intuitively indicate the size and distribution of conjugated π-bonds in the soluble oligomer. From part 2 (marked in Fig. 2), it can be seen that the conjugated π-bonds obtained from the polymerization of furfural was smaller than that of vanillin. Besides, the size of conjugated π-bonds produced by the mixture of furfural and vanillin was in between, which was resulted from the cross-polymerization between furfural and vanillin.

3.3. The relative molecular weight of the soluble oligomers

During the conversion of furfural and vanillin, different degree of polymerization occurred, resulting in polymers of varied molecular sizes and relative molecular weight. With the increase of degree of polymerization and relative molecular weight of polymers, insoluble oligomers were transformed into insoluble polymers. The relative molecular weight of liquid products measured by GFC can reflect the degree of polymerization to some extent. H_2SO_4 can significantly promote the polymerization of furfural and vanillin. The relative molecular weights of liquid products were 1784.4 and 1362.2 (Entry 1 and 6, Table 2), respectively. The cross-polymerization of furfural and vanillin increased the relative molecular weights of liquid products (Entry 11, Table 2). In addition, the acidity of the catalyst was proportional to the effect of catalytic polymerization, so the relative molecular weight of liquid product with acetic acid as catalyst was significantly smaller than that of other acids as catalyst. However, although strong alkali catalyzed polymerization, it was more likely to produce insoluble polymers. The relative molecular weight of liquid products was between 300 and 500.

3.4. FT-IR characterization of the liquid products and pastes

Figs. 3–4 show the FT-IR spectra of the liquid products and the pasty materials produced by the polymerization. Bending vibration of −OH was observed around 3400 cm^{-1}. Stretching of aliphatic −CH was observed around 2900 cm^{-1}. Aldehydes, carbonyls were observed at 1740 and 1700 cm^{-1}. Conjugated olefins and aromatic C=C were observed at 1600 and

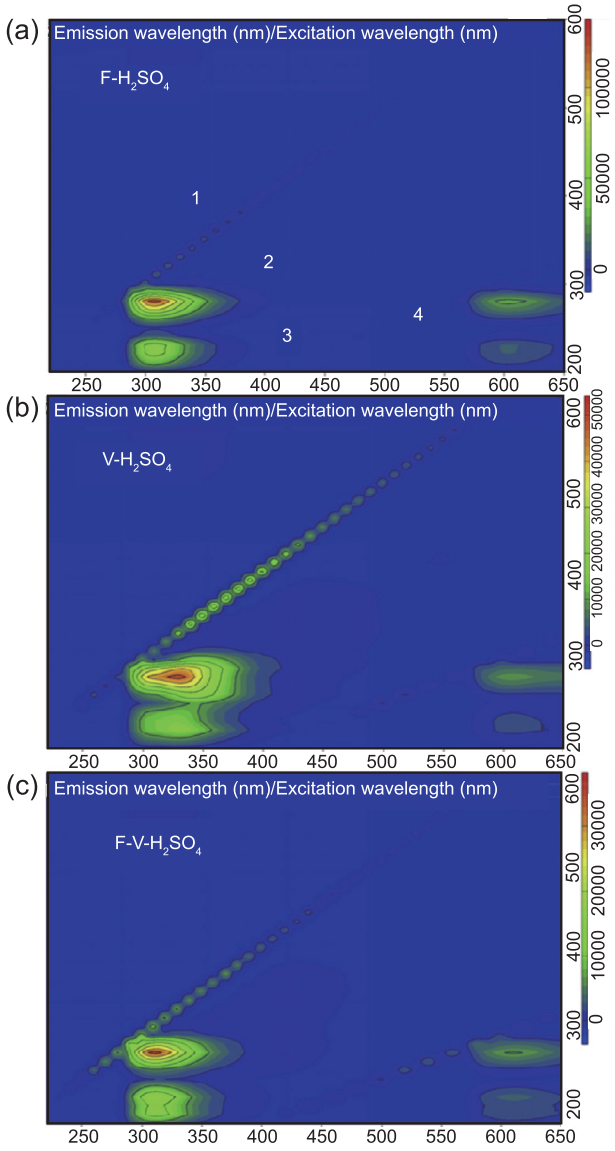

Fig. 2. 3D UV-fluorescence synchronous spectra of liquid products produced via the polymerization with H_2SO_4 as catalyst. The spectra are divided into four parts. Part 1 is Rayleigh scattering; Part 2 is conjugated π-bonds in the sample; Part 3 is the interaction between hydroxyl in conjugated π-bonds and H^+ in solvent; Part 4 is secondary signal (secondary projection of 2 and 3) [32]. (a) furfural as reactant; (b) vanillin as reactant; (c) the mixture of furfural and vanillin as reactant. All samples were diluted to 400 ppm by methanol.

1500 cm^{-1}, respectively. Aliphatic C–O stretching or deformation of furan rings were observed from 1270 to 1020 cm^{-1}. The characteristic peaks of the fingerprint region were the in-plane bending vibration of C–H in aromatic rings. The soluble polymers generally contained these functionalities, but their relative abundances were different.

Table S1 showed that the C=O/C=C ratio in the soluble oligomer changed greatly compared to that of precursor. The corresponding wavelengths of C=O and conjugated olefins C=C are 1700 and 1600 cm^{-1} respectively. The C=O/C=C ratio of the soluble polymer from furfural polymerization generally decreased when compared with that in furfural

Table 2
The relative molecular weight of the soluble oligomers.

Entry	Sample	Soluble oligomer M_w[a] (g mol^{-1})
1	F−H_2SO_4	1784.4
2	F−NaOH	488.7
3	F-FA	482.4
4	F-AA	226.2
5	F	113.4
6	V−H_2SO_4	1362.2
7	V−NaOH	369.5
8	V-FA	388.1
9	V-AA	142.1
10	V	140.7
11	F−V−H_2SO_4	1976.7
12	F−V−NaOH	386.6
13	F−V-FA	318.8
14	F−V-AA	110.0
15	F−V	106.6

[a] The average relative molecular weight determined by GFC.

feedstock (Entry 16, Table S1), which might be due to two reasons. Firstly, aldehyde could be consumed via the aldol addition/condensation, which produced additional C=C bonds. Taking furfural as an example, the mechanism of its aldol condensation was studied. In the hydrothermal process, the polymerization of furfural is accompanied by ring opening and bond breaking [33], resulting in a highly active intermediate. The aldehydes and carbonyls of C_1 and C_4 have three α-H (C_2, C_3 and C_5), so the aldol condensation reactions take place at C_2, C_3 and C_5 positions respectively. It is assumed that the aldehyde group in C_1 position will occur aldol condensation reactions in these three positions respectively, and the reaction mechanism was shown in Fig. S3. In addition, the carbonyls or aldehydes in C_4 and C_5 positions will also participate in the Aldol condensation, which will gradually increase the size of the polymer, and then form the insoluble polymer. Secondly, C=C bonds could also be formed via keto−enol tautomerism of the dehydrated species or intermolecular dehydration [37]. Besides, the FT-IR spectra of the polymer from the polymerization of furfural and vanillin were different, further indicating the existence of the interaction or the cross-polymerization between furfural and vanillin or their intermediates during the polymerization.

Comparing to that with H_2SO_4 as catalyst, the C=O/C=C ratio was much higher when NaOH was used as catalyst for the polymerization of vanillin (Entry 6 versus Entry 7 in Table S1). Aldol addition/condensation was more favorable under acidic conditions, and thus consuming more aldehydes and producing more C=C. For the pasty materials formed from polymerization of furfural (Entry 4 and 5, Table S1), the C=O/C=C was much higher than that in furfural feedstock, especially for the paste formed from the polymerization of furfural in the absence of catalysts, this further proved that the polymerization of furfural involved the opening of the furan ring in furfural and the consumption of more carbonyl functionalities in the polymerization. For the polymerisation of furfural or the

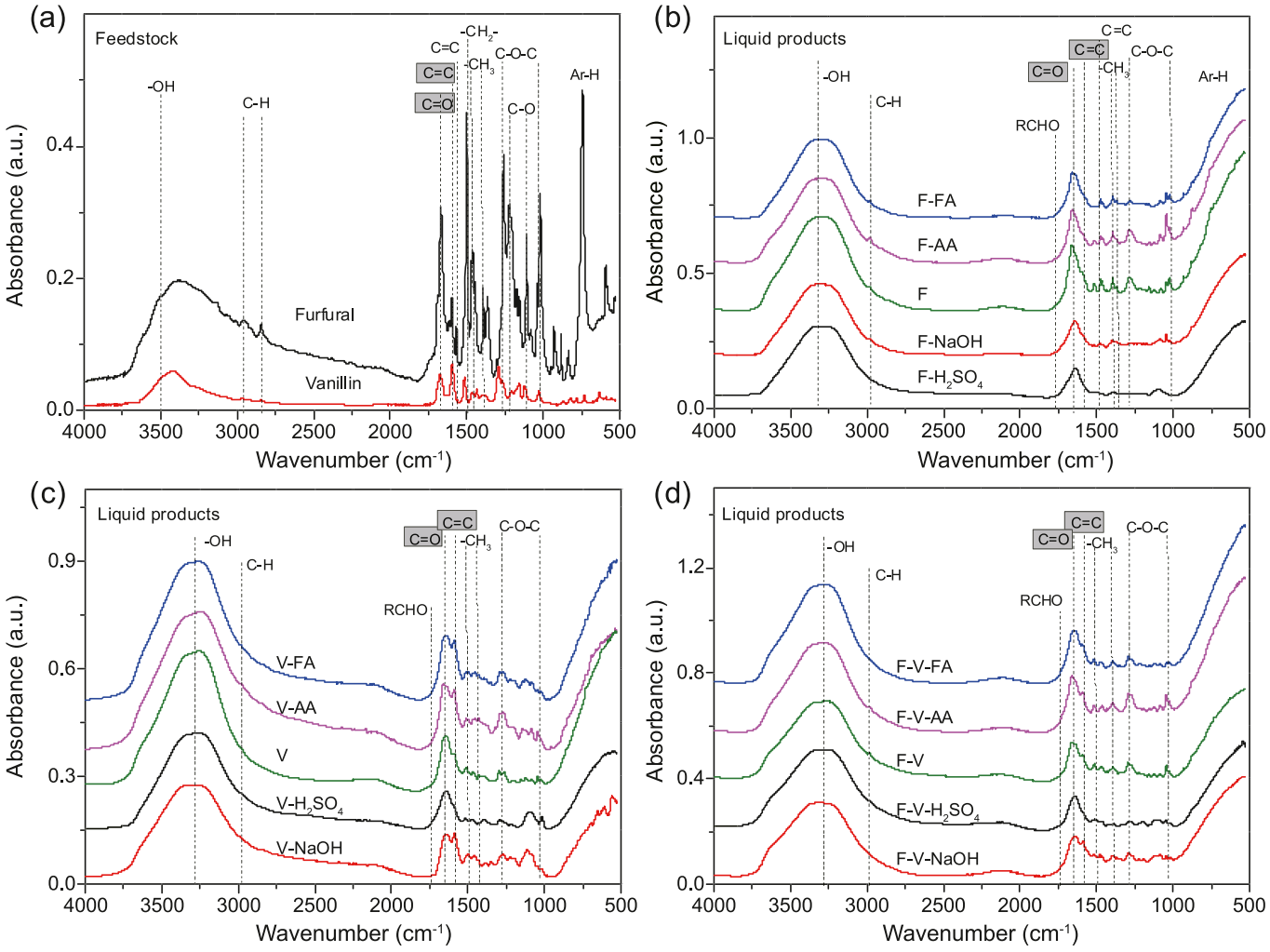

Fig. 3. FT-IR spectra of feedstock and liquid products produced via the polymerization. (a) Feedstock; (b) liquid products produced with furfural as reactant; (c) liquid products produced with vanillin as reactant; (d) liquid products produced with the mixture of furfural and vanillin as reactant.

mixture of furfural/vanillin with NaOH as catalyst, the C=O/C=C ratio was much lower than that with H_2SO_4 as catalyst (Entry 2 and 12 versus Entry 1 and 11 in Table S1), indicating that the presence of NaOH could facilitate the consumption of the carbonyl functionalities especially in furfural. H_2SO_4 as catalyst was more effectively for consumption of the carbonyl functionalities during the polymerization of vanillin.

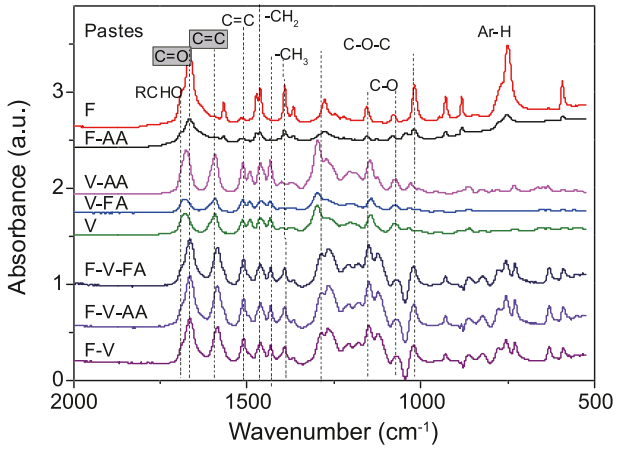

Fig. 4. FT-IR spectra of the pastes produced via the polymerization of furfural or/and vanillin.

3.5. The morphology of the polymers

The morphologies of the polymers formed were obviously different with the different precursors and the presence of different catalyst (Fig. 5). Carbonaceous spheres were formed from polymerization of furfural with sulfuric acid as catalyst (Fig. 5a). Opening of the furan ring in furfural produced the reactive intermediates bearing carbonyl functionalities [29], which further reacted via intermolecular aldol addition/condensation reactions, resulting in the formation of soluble oligomers. The aromatization of the soluble oligomers formed C=C through keto–enol tautomerism or intramolecular dehydration [38,39]. The aromatic clusters nucleated after reaching the critical supersaturation point. The formed nuclei further grew into carbonaceous spheres by

further condensation. The growth of carbonaceous spheres can be explained by a thin slice model, which showed that each carbonaceous sphere exhibited a core–shell structure consisting of a dense hydrophobic core and a hydrophilic shell [40–43]. The granular surface morphology was caused by the self-assembly of micro-carbon-containing spheres, which were obtained by the polymerization of furfural and their intermediates and subsequently into a larger spheres [40,42,44]. Thermodynamically, the surface energy of small carbonaceous spheres was high and thus the Ostwald ripening and agglomeration spontaneously occurred during hydrothermal carbonization.

In the presence of sulfuric acid, the polymerization of vanillin resulted in the formation of blocky solids with some stripe structures (Fig. 5c). It seems the polymerization of vanillin or the intermediates derived from vanillin proceeded quickly, forming the dense structures. With NaOH as catalyst, the surface of the blocky solids was rough (Fig. 5d). For the polymers formed from the polymerisation of furfural in the presence of NaOH, the polymer was also blocky particles with rough surface (Fig. 5b). The mechanism for the polymerisation

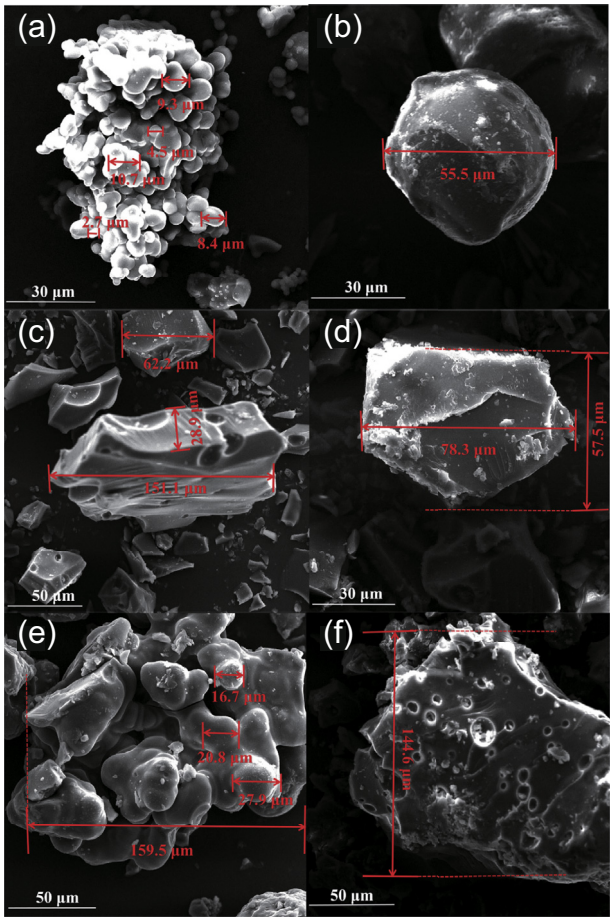

Fig. 5. SEM images of the polymer produced via the polymerization. (a) The polymerization of furfural with H_2SO_4 as catalyst; (b) the polymerization of furfural with NaOH as catalyst; (c) the polymerization of vanillin with H_2SO_4 as catalyst; (d) the polymerization of vanillin with NaOH as catalyst; (e) the polymerization of furfural and vanillin with H_2SO_4 as catalyst; (f) the polymerization of furfural and vanillin with NaOH as catalyst.

in the presence of H_2SO_4 or NaOH were clearly different in the polymerisation of whether furfural or vanillin. For the polymerization of the mixture of furfural and vanillin, with H_2SO_4 as catalyst the spheres merged (Fig. 5e), which was different from the polymer from vanillin or furfural itself, indicating the cross-polymerization between furfural and vanillin. With NaOH as catalyst, many dots in the blocky materials were observed (Fig. 5f), which was not presented in the polymer formed from vanillin or furfural in the presence of NaOH. Obviously, the mechanism for the cross-polymerization between furfural and vanillin was different from that of the single feedstock, which significantly affected the morphologies of the resulting polymer with sulfuric acid or NaOH as catalysts.

3.6. The solubility of the polymers in acetone

Table 3 shows the solubility of the solid polymer formed in the polymerization of furfural, vanillin or the mixture with acetone as the solvent. For the polymerization of furfural, the presence of NaOH or H_2SO_4 could obviously enhance the degree of the polymerization, as evidenced by the lower solubility of the solid polymer than that formed with formic acid or acetic acid as catalyst. In addition, whether with furfural or vanillin as feedstock, the polymer formed with H_2SO_4 as catalyst showed a lower stability than that with NaOH as catalyst. The solubility of the polymer produced from the polymerization of the mixture of furfural and vanillin, however, was relatively higher than that from the single feedstock. The cross-polymerization between furfural and vanillin clearly affected the structures of the resulting polymer. The GC–MS was used to characterize the extractives of polymers. The abundances of the organics were generally in trace level and thus were not present. Under the acidic conditions, furfural could be converted into small amount of levulinic acid, which has been reported in our previous studies [45]. In addition, the cracking of the side chain of vanillin was also observed, producing the compounds like guaiacol in the extractives.

3.7. FT-IR characterization of the polymers

The FT-IR spectra of the polymers produced via polymerization were showed in Fig. 6. The distribution of the functionalities was generally similar to that of the liquid products, except the formation of the carbonyl linked to unsaturated bonds at 1670 cm^{-1}. The polymerization of furfural or vanillin involves the formation or elimination of the C=O and C=C functionalities. It was believed that, during the polymerization, aldol addition/condensation reactions occurred, which consumed aldehyde functionality. Moreover, C=C of conjugated olefins may undergo 1,4 addition reactions. Meanwhile, the dehydration and intermolecular dehydration reactions could produce more C=O and C=C functionalities, respectively.

For the polymerization of furfural, C=O/C=C ratio is higher than 1 (except for NaOH as catalyst, Table S1), and hence the polymer was relatively rich in C=O. Nevertheless,

the C=O/C=C ratio is still lower than that in furfural feedstock (C=O/C=C ratio: 2.1). This result indicated that the polymerization of furfural involves the consumption of C=O functionality. In comparison, for the polymerization of vanillin, the C=O/C=C ratio is lower than 1, which was relatively rich in C=C (Table S1). This is understandable as vanillin contains more C=C bonds. In addition, the −CH out-of-plane deformation signals of vanillin polymerization showed an upward trend at about 850 cm^{-1}. These changes were attributed to the out-of-plane deformation of 1, 2, 4-trisubstituted aromatic rings [46]. For the polymerization of the mixture of furfural and vanillin, the C=O/C=C ratio is in between (except for NaOH as catalyst), and the substitution of aromatic and furan rings was weakened. Moreover, the aliphatic C–O stretching and C–H vibration of aromatic rings were significantly different. It also proved that the interaction (cross-polymerization) between furfural and vanillin or their intermediates occurred during the polymerization. In addition, the polymers produced from the polymerization of furfural are more open-ring conjugated structures, but the polymers produced from the polymerization of vanillin are more aromatic. And then, the polymers produced from the cross-polymerization of furfural and vanillin are more polycyclic structures. According to the difference of functionalities and structures of the polymers, the possible chemical structure model was given (Fig. S10).

The use of the acid catalyst and the alkaline catalysts significantly influenced the properties and structures of the polymers. The functionalities of the polymers obtained by acid catalysis were similar to those of without catalyst. Nevertheless, when NaOH was used as catalyst, a remarkably lower C=O/C=C ratio is obtained (Entry 7, Table S1). The aldehyde group was obviously consumed in large quantities under alkaline conditions, which produced more C=C. Alkali-catalyzed aldol addition/condensation was probably dominant during the polymerization, which was due to the different mechanisms of the aldol addition/condensation catalyzed by acids and alkalis. When acid was used as catalyst, the nucleophilic addition of enol anion was the nucleophilic addition of carbon anion, while alkaline catalyst catalyzed the nucleophilic addition of oxygen anion. Moreover, the opening of furan rings could produce more reactive intermediates with C=O functionalities, while, as mentioned above, benzene ring in vanillin was difficult to be opened. Furthermore, the cracking of vanillin molecules forms guaiacol without an aldehyde group, which also weakened the tendency for the occurrence of aldol addition/condensation, leading to a lower C=O/C=C ratio in the insoluble polymer formed.

Table 3
The solubility and the main extractives of the polymers[a].

Entry	Sample	Solubility (%)	Main extractives
1	F−H_2SO_4	1.3	furfural
2	F−NaOH	2.2	furfural
3	F-FA	9.2	furfural; levulinic acid
4	F-AA	8.5	furfural; acetic acid; 5-methyl-furfural
5	F	3.9	furfural; 5-methyl-furfural
6	V−H_2SO_4	1.7	guaiacol; vanillin; methylvanillin
7	V−NaOH	4.1	guaiacol; vanillin; methylvanillin; O-dimethoxybenzene
8	F−V−H_2SO_4	16.7	guaiacol; vanillin
9	F−V−NaOH	10.7	guaiacol; vanillin; methylvanillin; 3-buten-2-one,4-(4hydroxy-3-methoxyphenyl)-

[a] 0.15 g of polymer was dissolved in 3 g of acetone and stirred for 30 min. After that, the solid residual and liquid were filtered and separated. The undissolved polymer was dried at 35 °C for 4 h and its solubility was calculated after reaching a constant weight. Besides, the separated liquids were tested by GC–MS.

3.8. Characterization of the thermostability of the polymers with TGA

During polymerization, the catalysts not only impacted the yield of polymer, but also the thermostabilitiy of the structure (Fig. 7). Strong acid and alkali promoted the degree of polymerization. As shown in Fig. 7a, b and c, with the use of H_2SO_4 and NaOH as catalysts, the thermal stability of the

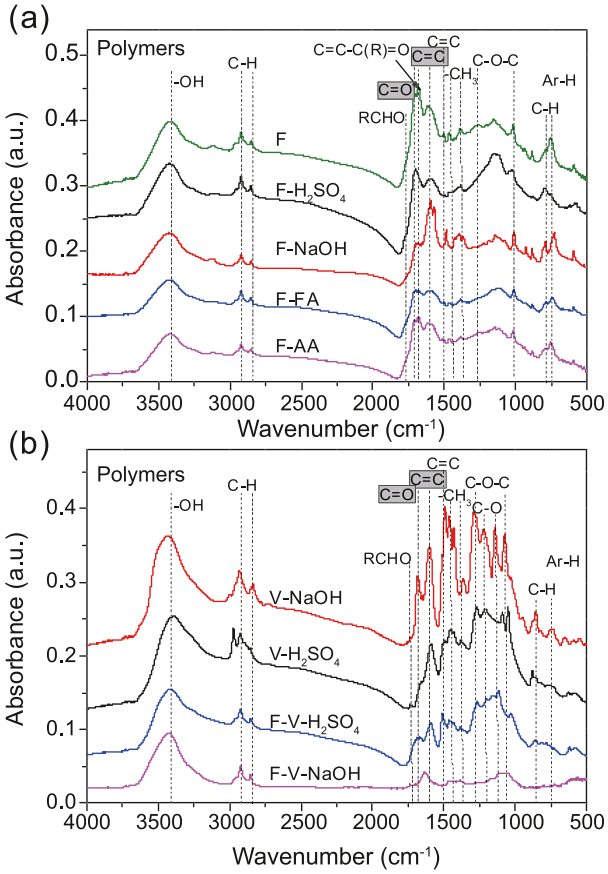

Fig. 6. FT-IR spectra of the polymers produced via the polymerization of the varied feedstock. (a) The polymers produced with furfural as reactant; (b) the polymers produced with vanillin and the mixture of furfural and vanillin as reactant.

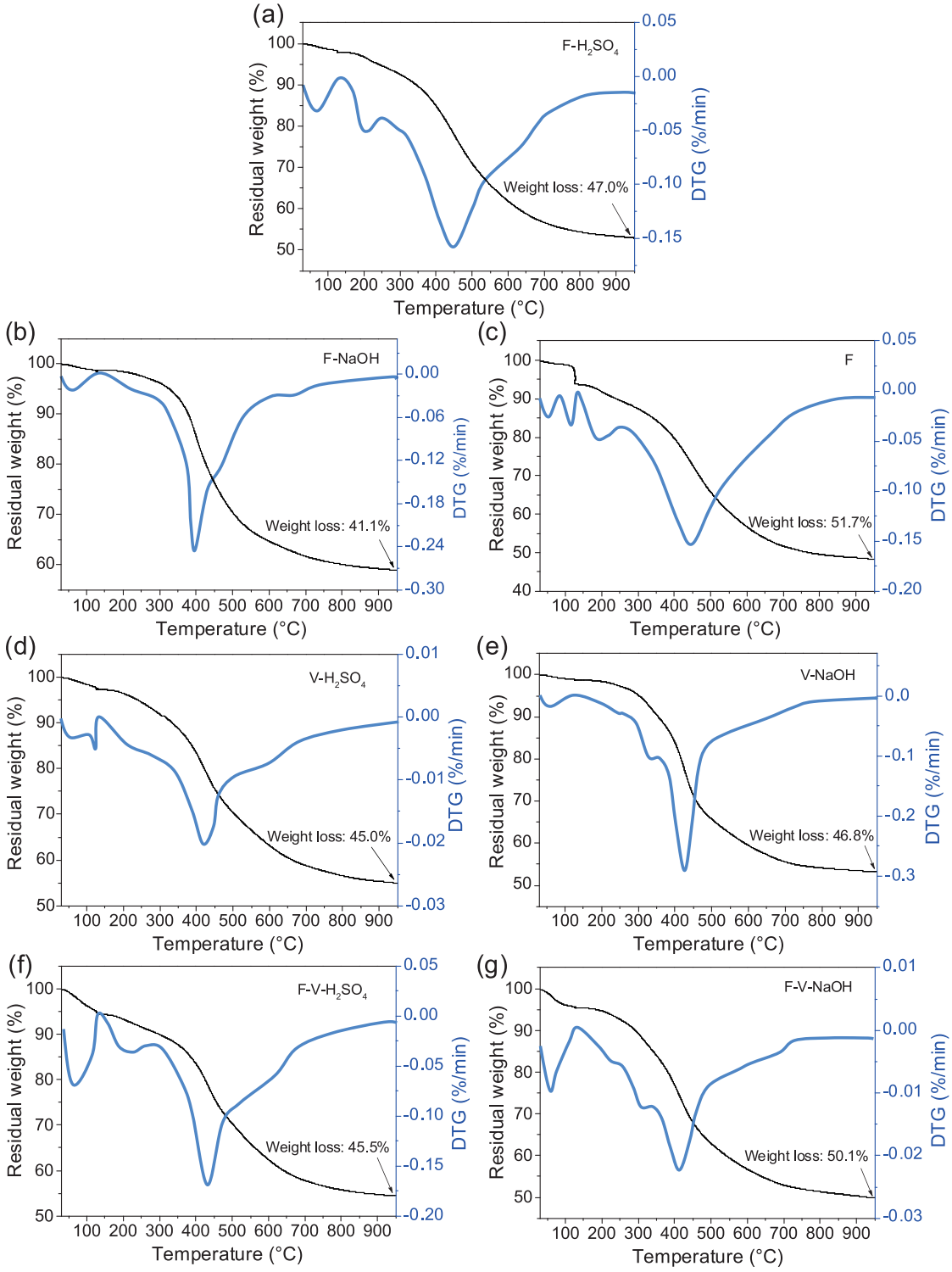

Fig. 7. TG/DTG curves of the polymers produced via the polymerization. (a)–(c) The polymers produced with furfural as reactant; (d) and (e) the polymers produced with vanillin as reactant; (f) and (g) the polymers produced with furfural and vanillin as reactant.

polymer was higher than that formed without a catalyst. NaOH as catalyst enhanced the polymerization via the aldol addition/condensation, improving the thermal stability of the polymer. Moreover, the formation of more C=C bonds further increased the stability of the polymer. For the polymer formed from the cross-polymerization between furfural and vanillin with H_2SO_4 as catalyst, the thermal stability of the polymers was similar to that from the single feedstock. In comparison, with NaOH as catalyst, the thermal stability of the polymer from furfural and vanillin was even lower. The results herein

indicated that the cross-polymerization between furfural and vanillin could increase the yields of the soluble polymer and also impact the formation of the functionalities on surface of the catalyst, but not necessarily increased the thermal stability of the polymer formed.

4. Conclusions

In summary, the results indicated that the polymerisation of furfural or vanillin was significantly affected by the catalysts. Acetic acid, as a weak organic acid, could catalyze the polymerisation of furfural to a pasty material, while formic acid with a higher acidity could further enhance the polymerisation of furfural to form solid polymers. The use of H_2SO_4 or NaOH could drastically enhance the degree of the polymerization of furfural due to their strong acidity/alkalinity. Vanillin showed a higher tendency towards polymerization than furfural, which was probably related to the bigger π-conjugated ring structures in vanillin. The polymerisation of vanillin was not affected much by the organic acids, while, similarly, the presence of H_2SO_4 or NaOH significantly enhanced the degree of polymerization of vanillin by shifting the pasty material to solid polymer. The cross-polymerization between furfural and vanillin did exist, which could cross-polymerize even in the absence of catalyst, enhancing the overall yield of the polymer formed. In the presence of H_2SO_4 or NaOH, the cross-polymerization between furfural and vanillin led to the formation of more solid polymer than that from the polymerisation of the individual furfural or vanillin feedstock. The polymerisation of furfural associates with the consumption of the carbonyl functionalities in the reaction intermediates formed from the degradation of furfural via aldol addition/condensation reactions, especially with NaOH as catalyst. Similar phenomenon was not observed for the polymerization of vanillin, resulting from their varied routes for the polymerisation. In addition, the acid/alkaline catalysts and the cross-polymerization between furfural and vanillin showed substantial influences on morphology and thermostability of the resulting polymers. Besides vanillin, there are a number of phenolics in bio-oil with varied functionalities and structures. The cross-polymerization between furfural and these phenolics needs further investigation, aiming to establish the correlation of the tendency towards polymerization with the structural configuration of these organics.

Conflict of interest

The authors declare no conflict of interest.

Acknowledgements

This work was supported by the National Natural Science Foundation of China (No. 51876080), Australian Research Council (ARC) Discovery Project scheme (DP180101788), the Australian Government through ARENA's Emerging Renewables Programs, the Strategic International Scientific and Technological Innovation Cooperation Special Funds of National Key R&D Program of China (No. 2016YFE0204000), the Program for Taishan Scholars of Shandong Province Government, the Recruitment Program of Global Young Experts (Thousand Youth Talents Plan), the Natural Science Fund of Shandong Province (ZR2017BB002) and the Key R&D Program of Shandong Province (2018GSF116014).

Appendix A. Supplementary data

Supplementary data to this article can be found online at https://doi.org/10.1016/j.gee.2020.03.009.

References

[1] S.S. Toor, L. Rosendahl, A. Rudolf, Energy 36 (2011) 2328–2342.
[2] M.F. Demirbas, Appl. Energy 86 (2009) S151–S161.
[3] S. Zhou, T.M. Runge, Carbohydr. Polym. 112 (2014) 179–185.
[4] D.M. Alonso, S.G. Wettstein, J.A. Dumesic, Chem. Soc. Rev. 41 (2012) 8075–8098.
[5] B.R. Caes, R.E. Teixeira, K.G. Knapp, R.T. Raines, ACS Sustain. Chem. Eng. 3 (2015) 2591–2605.
[6] N.A.S. Ramli, N.A.S. Amin, Fuel Process. Technol. 128 (2014) 490–498.
[7] F. Wei, J.P. Cao, X.Y. Zhao, J. Ren, B. Gu, X.Y. Wei, Fuel 218 (2018) 148–154.
[8] S. Kang, J. Fu, G. Zhang, Renew. Sustain. Energy Rev. 94 (2018) 340–362.
[9] X. Hu, S. Wang, L. Wu, D. Dong, M.M. Hasan, C.-Z. Li, Fuel Process. Technol. 126 (2014) 315–323.
[10] H. Chen, J. Liu, X. Chang, D. Chen, Y. Xue, P. Liu, H. Lin, S. Han, Fuel Process. Technol. 160 (2017) 196–206.
[11] Y. Zhang, X. Chen, X. Lyu, G. Zhao, T. Zhao, L. Han, W. Xiao, J. Clean. Prod. 215 (2019) 712–720.
[12] X. Hu, C. Lievens, D. Mourant, Y. Wang, L. Wu, R. Gunawan, Y. Song, C.Z. Li, Appl. Energy 111 (2013) 94–103.
[13] D. Mohan, C.U. Pittman, P.H. Steele, Energy Fuels 20 (2006) 848–889.
[14] Y. Wang, X. Li, D. Mourant, R. Gunawan, C.Z. Li, Energy Fuels 26 (2011) 241–247.
[15] R. Gunaw. an, X. Li, A. Larcher, X. Hu, D. Mourant, W. Chaiwat, H. Wu, C.-Z. Li, Fuel 95 (2012) 146–151.
[16] Y. Wang, D. Mourant, X. Hu, S. Zhang, C. Lievens, C.Z. Li, Fuel 108 (2013) 439–444.
[17] A. Demirbas, Fuel Process. Technol. 88 (2007) 591–597.
[18] Y. Ma, G. Xu, H. Wang, Y.X. Wang, Y. Zhang, Y. Fu, ACS Catal. 8 (2018) 1268–1277.
[19] X. Hu, Y. Wang, D. Mourant, R. Gunawan, C. Lievens, W. Chaiwat, M. Gholizadeh, L. Wu, X. Li, C.Z. Li, AIChE J. 59 (2013) 888–900.
[20] W. Yu, Y. Tang, L. Mo, P. Chen, H. Lou, X. Zheng, Catal. Commun. 13 (2011) 35–39.
[21] W. Chaiwat, R. Gunawan, M. Gholizadeh, X. Li, C. Lievens, X. Hu, Y. Wang, D. Mourant, A. Rossiter, J. Bromly, C.Z. Li, Fuel 112 (2013) 302–310.
[22] S. Czernik, A.V. Bridgwater, Energy Fuels 18 (2004) 590–598.
[23] X. Hu, S. Jiang, L. Wu, S. Wang, C.Z. Li, Chem. Commun. 53 (2017) 2938–2941.
[24] G.W. Huber, S. Iborra, A. Corma, Chem. Rev. 106 (2006) 4044–4098.
[25] Z. Zhang, Q. Wang, X. Yang, S. Chatterjee, C.U. Pittman, Green Chem. 13 (2011) 940–949.
[26] A. Gaurav, F.T.T. Ng, G.L. Rempel, Green Energy Environ. 1 (2016) 62–74.
[27] S. Suttibak, K. Sriprateep, A. Pattiya, Energy Sources, Part A 37 (2015) 1440–1446.
[28] C.Z. Li, X. Hu, Australian Patent (2016). Publication No.: WO/2016/164965.
[29] X. Hu, K. Nango, L. Bao, T. Li, M.M. Hasan, C.Z. Li, Green Chem. 21 (2019) 1128–1140.

[30] X. Hu, S. Kadarwati, S. Wang, Y. Song, M.M. Hasan, C.Z. Li, Fuel Process. Technol. 137 (2015) 212–219.
[31] S.F. Hashmi, H. Meriö-Talvio, K.J. Hakonen, K. Ruuttunen, H. Sixta, Fuel Process. Technol. 168 (2017) 74–83.
[32] Q. Xu, X. Hu, Y. Shao, K. Sun, P. Jia, L. Zhang, Q. Liu, Y. Wang, S. Hu, J. Xiang, Carbohydr. Polym. 216 (2019) 167–179.
[33] X. Hu, R. Westerhof, D. Dong, L. Wu, C.Z. Li, ACS Sustain. Chem. Eng. 2 (2014) 2562–2575.
[34] S. Zheng, F. Jin, Y. Zhang, B. Wu, A. Kishita, K. Tohji, H. Kishida, AIChE J. 48 (2009) 2727–2733.
[35] M.J. Climent, A. Corma, S. Iborra, A. Velty, Catal. Lett. 79 (2002) 157–163.
[36] Y. Shao, X. Hu, Z. Zhang, K. Sun, G. Gao, T. Wei, S. Zhang, S. Hu, J. Xiang, Y. Wang, Green Energy Environ. 3 (2018) 1–14.
[37] M. Sevilla, A.B. Fuertes, Chem. Eur J. 15 (2009) 4195–4203.
[38] J. Ryu, Y.W. Suh, D.J. Suh, D.J. Ahn, Carbon 48 (2010) 1990–1998.
[39] M.M. Tang, R. Bacon, Carbon 2 (1964) 221–225.
[40] G.H. Moon, Y. Shin, B.W. Arey, C. Wang, G.J. Exarhos, W. Choi, J. Liu, Colloid Polym. Sci. 290 (2012) 1567–1573.
[41] B. Hu, K. Wang, L. Wu, S.H. Yu, M. Antonietti, M.M. Titirici, Adv. Mater. 22 (2010) 813–828.
[42] C. Yao, Y. Shin, L.Q. Wang, C.F. Windisch, W.D. Samuels, B.W. Arey, C. Wang, W.M. Risen, G.J. Exarhos, J. Phys. Chem. C 111 (2007) 15141–15145.
[43] Q. Xu, L. Zhang, K. Sun, Y. Shao, H. Tian, S. Zhang, Q. Liu, G. Hu, S. Wang, X. Hu, J. Energy Inst. 93 (2020) 1678–1689.
[44] Y. Shin, L.Q. Wang, I.T. Bae, B.W. Arey, G.J. Exarhos, J. Phys. Chem. C 112 (2008) 14236–14240.
[45] X. Hu, C. Lievens, C.Z. Li, ChemSusChem 5 (2012) 1427–1434.
[46] I. Zandvoort, Y. Wang, C.B. Rasrendra, R.H. Eck, C.A. Bruijnincx, J. Heeres, M. Weckhuysen, ChemSusChem 6 (2013) 1745–1758.